Soft Materials

ISSN: (Print) (Online) Journal homepage: https://www.tandfonline.com/loi/lsfm20

Biocompatible, stretchable, and compressible cellulose/MXene hydrogel for strain sensor and electromagnetic interference shielding

Yan Bai, Shuaihang Bi, Weikang Wang, Ning Ding, Yuyuan Lu, Mengyue Jiang, Chengbo Ding, Weiwei Zhao, Ning Liu, Jing Bian, Shujuan Liu & Qiang Zhao

To cite this article: Yan Bai, Shuaihang Bi, Weikang Wang, Ning Ding, Yuyuan Lu, Mengyue Jiang, Chengbo Ding, Weiwei Zhao, Ning Liu, Jing Bian, Shujuan Liu & Qiang Zhao (2022): Biocompatible, stretchable, and compressible cellulose/MXene hydrogel for strain sensor and electromagnetic interference shielding, Soft Materials, DOI: 10.1080/1539445X.2022.2081580

To link to this article: https://doi.org/10.1080/1539445X.2022.2081580

SOFT MATERIALS
https://doi.org/10.1080/1539445X.2022.2081580

Biocompatible, stretchable, and compressible cellulose/MXene hydrogel for strain sensor and electromagnetic interference shielding

Yan Bai, Shuaihang Bi, Weikang Wang, Ning Ding, Yuyuan Lu, Mengyue Jiang, Chengbo Ding, Weiwei Zhao, Ning Liu, Jing Bian, Shujuan Liu, and Qiang Zhao

State Key Laboratory of Organic Electronics and Information Displays & Jiangsu Key Laboratory for Biosensors, Institute of Advanced Materials (IAM) & Institute of Flexible Electronics (Future Technology), Nanjing University of Posts & Telecommunications, Nanjing, Jiangsu, China; College of Electronic and Optical Engineering & College of Microelectronics, Jiangsu Province Engineering Research Center for Fabrication and Application of Special Optical Fiber Materials and Devices, Nanjing University of Posts and Telecommunications (NUPT), Nanjing, Jiangsu, China

ABSTRACT

With the booming growth of flexible human-computer interactions and telecommunications, it is desirable to fabricate a high-sensitivity strain sensor to monitor human movement and develop an electromagnetic interference (EMI) shielding materials to protect modern microelectronics and humans from electromagnetic damage. Herein, the biocompatible, stretchable, and compressible cellulose/MXene hydrogel has been prepared to first realize the dual-functional applications in strain sensor and EMI shielding. Two-dimensional MXene nanosheets serve as conductive sensing materials and fillers to construct conductive networks. The hydrogen bond interaction between them enhances the mechanical property of hydrogel. Benefiting from the excellent electrical conductivity and good mechanical property of the cellulose/MXene hydrogel, the resultant strain sensor displays excellent tensile strain (~144.4%), high sensitivity (gauge factor ~ -6.97), adjustable detection range (0-68.7%), fast response time (~100 ms), and great stability (~1000 cycles). It can monitor human motion, including pulse beating, speech recognition, writing sensing and pressure distribution induction of 4 × 4 sensor array platform. Moreover, the cellulose/MXene hydrogel presents an absorption-predominant EMI shielding performance in the frequency of X-band. This work provides a new inspiration for the development of multifunctional hydrogel in artificial intelligence, human-computer interaction, and EMI shielding technique.

ARTICLE HISTORY
Received 27 January 2022
Accepted 20 May 2022

KEYWORDS
MXene; cellulose; hydrogel; strain sensor; electromagnetic interference shielding

Introduction

With the foreseeable prosperity of artificial intelligence and telecommunications, the wearable electronics have been widely used in health clinical monitoring,[1] soft robots,[2] electronic skin,[3] and other fields.[4,5] Among them, the flexible strain sensor can experience the ingenious conversion of the external strain stimulus into visible electrical signals, thus possessing the superior capability in real-time monitoring and human-computer interactions.[6,7] To meet the practical application, the key sensing constitutes should have both great biocompatibility and excellent mechanical property in principle. At present, the rapid innovation of electronic communication technology has brought negative problems of electromagnetic pollution, which interferes the electronic component to cause inaccurate signal as well as seriously affects the human health.[8] Therefore, it is of great significance to explore novel sensing materials for dual-functional applications in high-performance sensor and electromagnetic interference (EMI) shielding.

MXene is the emerging two-dimensional (2D) transition-metal carbides, nitrides, and carbonitrides with the merits of abundant hydrophilic surface groups (i.e., -O, -F, and -OH), large specific surface area, ultrahigh conductivity (1×10^4 S cm^{-1}) and excellent dispersion.[9–14] To date, MXene-based composite hydrogels prepared through the dispersion of MXene into elastic matrix (i.e. polyvinyl alcohol (PVA),[15] polydimethylsiloxane (PDMS)[16] and polyacrylamide (PAAM)[17]) has become a feasible strategy to construct strain sensor under complex deformation. However, considering the expectations of biocompatibility and environmental friendliness, it becomes a trend to explore the natural and renewable elastic polymer matrix.[18,19] As an almost inexhaustible and nontoxic polymer, cellulose is

CONTACT Weiwei Zhao iamwwzhao@njupt.edu.cn; Qiang Zhao iamqzhao@njupt.edu.cn State Key Laboratory of Organic Electronics and Information Displays & Jiangsu Key Laboratory for Biosensors, Institute of Advanced Materials (IAM) & Institute of Flexible Electronics (Future Technology), Nanjing University of Posts & Telecommunications, Nanjing, Jiangsu, China
Supplemental data for this article can be accessed online at https://doi.org/10.1080/1539445X.2022.2081580

a hopeful substitute to load conductive MXene fillers for the fabrication of cellulose/MXene hydrogel, which would be an ideal candidate for the strain sensors based on the adjustable three-dimensional (3D) conductive network, porous structure and mechanical property.[20–22] Moreover, the additional internal water-rich environment is expected to endow the cellulose-based hydrogels with the EMI shielding performance.[23] For example, the polyacrylamide (PAM)/cellulose nanofiber/multiwalled carbon nanotubes composite hydrogel shows high EMI shielding performance due to the pore structure and excellent conductivity to reflect, multi-reflect, and absorb the electromagnetic wave.[24] However, it is still rarely reported to evoke the dual-functional application of cellulose/MXene hydrogel in the field of strain sensor and EMI shielding.

Herein, the biocompatible, stretchable, and compressible cellulose/MXene hydrogel is first explored for the dual functional application in strain sensor and EMI shielding. The abundant surface groups (i.e., -O, -F, and -OH) of MXene nanosheets can cross-link the hydroxyl groups of cellulose through hydrogen bonds. MXene is embedded into the hydrogel as fillers to improve the mechanical property and effectively construct conductive networks. The cellulose/MXene hydrogel exhibits high conductivity, great stretchability, compressibility, and biocompatibility for the application of strain sensor. As a result, the strain sensor exhibits high sensitivity (GF = −6.97), excellent stretchability (~144.4%), compressibility (0-68.7%), and good stability (~1000 cycles). The outstanding performances enable it to monitor both large and subtle activities of human motion in real-time, recognize character, and monitor pressure distribution. Moreover, benefiting from appropriate conductivity, 3D porous structure, and abundant water content, it reveals the absorption-dominant EMI shielding effectiveness (SE) of 30 dB at 8.2 GHz.

Materials and Methods

Materials

α-cellulose, urea, epichlorohydrin (EPI), dimethyl sulfoxide (DMSO), and lithium fluoride (LiF) were purchased from Aladdin Reagent Company. Ti_3AlC_2 was commercially obtained from Nanjing Mingshan New Material Technology Co., Ltd. hydrochloric acid (HCl) and sulfuric acid (H_2SO_4) were obtained from Nanjing Chemical Reagent Co., Ltd. sodium hydroxide (NaOH) was purchased from Xilong Science Co., Ltd. HeLa cells were purchased from the Institute of Biochemistry and Cell Biology, SIBS, CAS. Dulbecco's modified Eagle's medium (DMEM) and fetal bovine serum (FBS) were supplied from Beyotime Biotechnology.

Fabrication of cellulose-based Hydrogel

Firstly, cellulose powder was dissolved in NaOH/urea (7 wt%:12 wt%) aqueous solution and frozen to prepare cellulose solution (4 wt%). Then, cellulose solution was added to MXene with different concentrations of 0, 2.5, 5, 7.5, 10, 20, 30, 40, and 50 mg mL^{-1}. Subsequently, epichlorohydrin (EPI) crosslinking agent was added to the mixture and stirred for 20 min. The hydrogel was formed after the reaction for 2 h at 45°C. Then, they were immersed in H_2SO_4 solution to terminate the chemical crosslinking reaction. Finally, the deionized water was used to thoroughly wash the hydrogel to remove the impurities after reaction until the pH value reached 7.

Assembly and Sensing Test of cellulose/MXene Hydrogel

The strain sensing test was performed by attaching copper tape on the upper and lower sides of the hydrogel, and connecting to the electrochemical workstation through wires. The tensile tester applies pressure to obtain a real-time current signal at a constant voltage of 1 V. The two sides of the hydrogel were pasted with copper foil through the VHB film on the skin and fixed with tape to test human activities.

EMI Shielding Test of cellulose/MXene Hydrogel

According to the Institute of Electrical and Electronic Engineers Standard 521, the X-band is defined as the radio wave band with a frequency of 8-12 GHz.[25] The EMI SE of the cellulose/MXene hydrogel (30 × 30 mm^2) was measured by the vector network analyzer (Keysight E5071C) in 8.2–12.4 GHz (X band). It was calculated from the scattering parameters (S_{11} and S_{21}) by the following equation[26]:

$$SE_T = SE_R + SE_A + SE_M \quad (1)$$

$$SE_R = -10\log\left(1 - |S_{11}|^2\right) \quad (2)$$

$$SE_A = -10\log\left(\frac{|S_{21}|^2}{\left(1 - |S_{11}|^2\right)}\right) \quad (3)$$

where SE_T is the total SE, SE_R is the reflection SE and SE_A absorption SE. SEM is the multiple reflections shielding, which will negligible when $SE_T \geq 15$ dB.[24]

Results and Discussion

Preparation and Characterization of cellulose/MXene Hydrogel

The synthesis route of the cellulose/MXene hydrogel is shown in Figure 1a and Figure. S1. Ultrathin 2D MXene nanosheets are obtained by the ultrasonication of multi-layered MXene bulks (Figure 1a,b and Figure. S2).[27] The homogeneous dispersion of cellulose suspension is the precondition to achieve the uniform 3D networks in cellulose/MXene hydrogel. Cellulose powder is first dissolved in NaOH/urea aqueous solution. NaOH can destroy the intramolecular and intermolecular hydrogen bonds of cellulose. The urea can effectively break the intermolecular hydrogen bonds of polysaccharide polymers to accelerate the dissolution (Figure S3). The electrostatic interaction between cellulose and MXene benefits to disperse the MXene, and cellulose as a dispersant effectively avoids the agglomeration of MXene (Figure S4). EPI is cross-linked with -OH groups of cellulose to form the hydrogel. Furthermore, the abundant functional groups (i.e., -O, -F, and -OH) of MXene can be immobilized in the hydrogel through hydrogen bond interactions with the hydroxy functional group of cellulose.[21] The hydrogen bond interactions also exist in the intramolecular or intermolecular of cellulose.[28]

The cellulose/MXene hydrogel can quickly recover to the initial state after stretching or compressing, indicating its mechanical resilience (Figure 1c). The various shapes of hydrogel can be designed through different molds, indicating its good shapeability (Figure 1d).

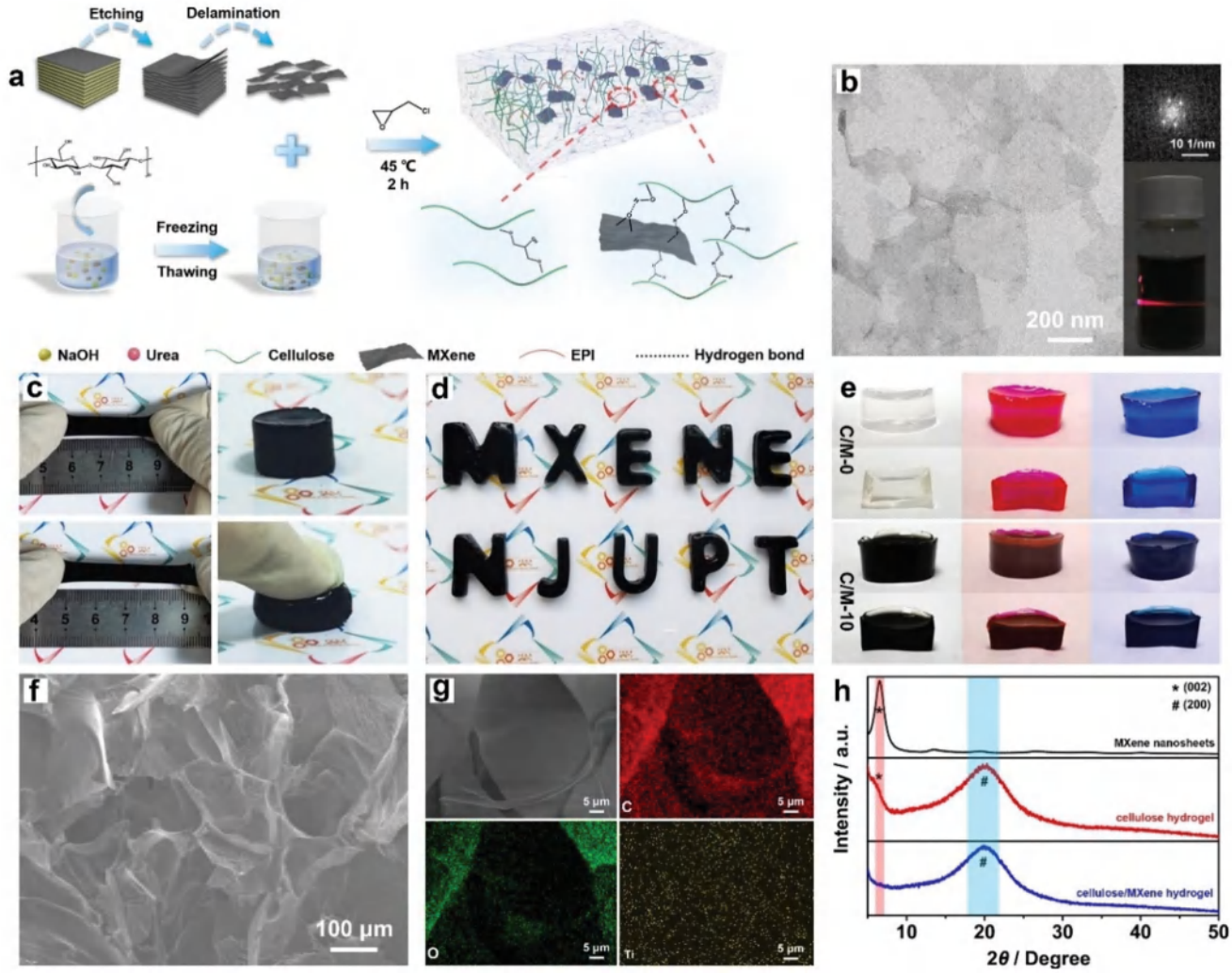

Figure 1. (a) Schematic illustration of the cellulose/MXene hydrogel. (b) TEM image of MXene nanosheets. Inset: the corresponding SAED image and photograph of Tyndall effect of MXene suspension. Photographs of the cellulose/MXene hydrogel with stretchability and compressibility (c) and shapeability (d). (e) Photographs of cellulose hydrogel and cellulose/MXene hydrogel adsorbing rhodamine (middle red) and methylene blue (right blue). SEM image (f) and EDS images (g) of cellulose/MXene hydrogel for C, O and Ti. (h) XRD patterns of MXene nanosheets, cellulose hydrogel and cellulose/MXene hydrogel.

Subsequently, cellulose hydrogel and cellulose/MXene hydrogel are immersed in rhodamine and methylene blue, respectively. They can be dyed uniformly red and blue in their interior (Figure 1e). It confirms that both cellulose hydrogel and cellulose/MXene hydrogel have well-maintained porous structure for adsorption (Figure 1f). The energy dispersive spectrometer (EDS) mapping images demonstrate that C, O and Ti elements uniformly distribute in the 3D networks (Figure 1g). The C and O elements are derived from cellulose and MXene, while Ti element is only assigned to MXene, indicating the even distribution of MXene nanosheets in the networks. X-ray diffraction (XRD) pattern confirms cellulose/MXene hydrogel contains both the characteristic peak of cellulose and MXene (Figure 1h). The (002) diffraction peak of cellulose/MXene hydrogel has shifted to a lower angle, which indicates that the 3D networks can effectively inhibit the aggregation of MXene.[29] These results show that cellulose is used as a dispersant and 3D network skeleton and MXene is embedded as a filler.

Performance Investigation

Cellulose as the 3D support framework plays a dominant role in the mechanical property of cellulose/MXene hydrogels. Considering the practical application, the hydrogel needs to have large strain variable, the cellulose concentration of 4 wt% is selected as the optimal addition amount (Figure S5 and Video S1). MXene is embedded in the hydrogel as a filler. The effects of MXene loading on the interior structure, gelling time, conductivity viscoelasticity, swelling ratio, and mechanical properties of the hydrogel are systematically explored. The cellulose/MXene hydrogels with different concentrations of MXene (i.e., 0, 2.5, 5, 7.5, 10, 20, 30, 40, and 50 mg mL^{-1}) are named as C/M-0, C/M-2.5, C/M-5, C/M-7.5, C/M-10, C/M-20, C/M-30, C/M-40 and C/M-50, respectively (Figure 2a). C/M-0 appears to be transparent, while the cellulose/MXene composite hydrogels turn black as MXene nanosheets are added. It indicates that the addition of MXene nanosheets has a significant effect on the transmittance of hydrogel. In order to explore the influence of MXene loading on the morphology of the hydrogel, we monitor the state before and after the formation of hydrogel (Figure S6). With the increase of MXene concentration, the number of black flocculent substances gradually increases, showing that the excessive MXene will cause the uneven distribution and agglomeration. SEM images are further verifying the results that the MXene addition of 0, 2.5, 5, 7.5, 10, and 20 mg mL^{-1} has no obvious effect on the formation of the pore structure (Figure S7). As the amount of MXene increases to 30 mg mL^{-1}, the stacking of MXene nanosheets appears. C/M-40 and C/M-50 show serious accumulation of MXene nanosheets, demonstrating that the excessive MXene concentration leads to the self-accumulation. Therefore, the samples of C/M-0, C/M-2.5, C/M-5, C/M-7.5, C/M-10, C/M-20, and C/M-30 are used for subsequent performance tests. In addition, as the amount of MXene increases from 0 to 30 mg L^{-1}, the gelation time of the hydrogel gradually becomes shorter (Figure S8). According to the concentration gradient, C/M-30 ~ C/M-0 are converted into hydrogel within 120 min, successively. It is ascribed to that the enhanced hydrogen bond interaction between MXene and cellulose accelerates the gelling rate.[21] The conductivity of C/M-0 is 9.1 mS m^{-1} due to the existence of Na^{+}.[30] The conductivity significantly increases as 11.5, 12.9, 14, 14.9, 16.2, and 18.8 mS m^{-1} for C/M-2.5, C/M-5, C/M-7.5, C/M-10, C/M-20, C/M-30, respectively (Figure 2b), which is higher than those in the previous works (Table S1). In this system, the improved amount of MXene causes more conductive pathways in the 3D networks to increase the conductivity.

The viscoelasticity behavior of hydrogel is investigated by the rheological measurements. A significant characteristic of hydrogel is that the storage modulus (G') is higher than the loss modulus (G") and maintain stable, showing the elastic solid performance.[31] The G′ and G″ of C/M-10 hydrogel are higher than C/M-0 hydrogel, indicating that the mechanical property is obviously improved (Figure 2c). The addition of MXene will enhance the degree of cross-linking with cellulose chain to improve the strength of hydrogel. The swelling ratio of C/M-0 and C/M-10 further reflects the molecular interactions between cellulose and MXene. C/M-0 is higher than C/M-10 (Figure 2d), indicating that the complex and staggered structure inhibit the absorption of water molecules. The tensile and compressive tests are carried out to confirm the effect of MXene loading on the mechanical property of hydrogel (Figure 2e,f and Table S2). With the amount of MXene increases from 0 to 10 mg mL^{-1}, the tensile failure strain raises from 101.6% to 144.4%. While as the addition of MXene increases to 20 and 30 mg mL^{-1}, the tensile failure strain decreases to 106.8% and 88.8%, respectively. The optimal value of C/M-10 is higher than other hydrogels in the previous works (Table S3). The Young's modulus increases significantly from 3.64 to 9.46 kPa with the amount of MXene increases from 2.5 to 30 mg mL^{-1}, indicating that MXene can enhance the rigidity of hydrogel. MXene is embedded in 3D skeleton through hydrogen bond interaction to improve the tensile property and mechanical strength of hydrogel. However, the excessive MXene concentration over

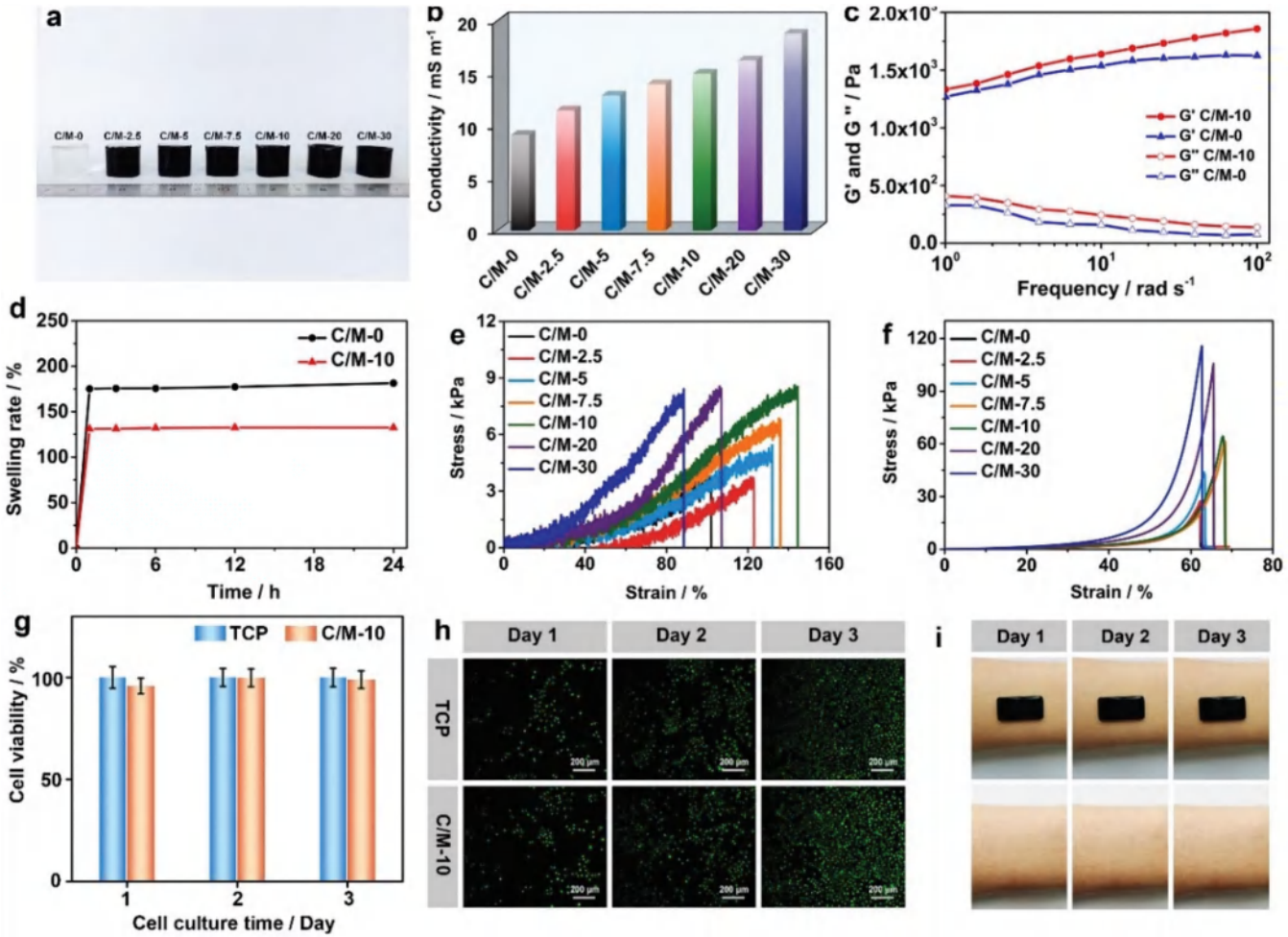

Figure 2. Performance analysis of the hydrogel. The photographs (a) and conductivity (b) of C/M-0, C/M-2.5, C/M-5, C/M-7.5, C/M-10, C/M-20 and C/M-30. Rheological (c) and swelling (d) properties of C/M-0 and C/M-10. The stretchability (e) and compressibility (f) of hydrogel with different MXene content. (g) Cell viability of HeLa cells culture after 1, 2, and 3 d with TCP and hydrogels. (h) LIVE/DEAD staining of HeLa cells after incubating with hydrogels and TCP for 3 d. (i) The photographs of skin test with hydrogel direct contacting on human wrist for 1, 2 and 3d.

10 mg mL^{-1} will hinder the effective slippages of cellulose to decrease the tensile failure strain. The situation also appears in the compression test. As the amount of MXene increases from 0 to 30 mg mL^{-1}, the compression failure strain first raises and then decreases. C/M-10 has the maximum compression deformation of 68.7%, and the compression stress continuously increases from 25 to 116.1 kPa with MXene addition improving from 0 to 30 mg mL^{-1}, which is higher than those in the previous works (Table S4). As a kind of nanofillers, MXene compacts the structure as the amount increases to improve the compressive strain and strength.[32,33] However, the compression failure strain decreases as the MXene concentration further increases, which is attributed to the aggregation of the MXene.[34] Here, it is noted that cellulose/MXene hydrogel with the MXene concentration of 10 mg mL^{-1} has the largest tensile and compression strain, which is also superior to other conventional 2D materials (Table S5). As a result, C/M-10 is selected for further research in strain sensor.

The biocompatibility experiments are carried out to explore the possibility of hydrogel in direct contact with the human body. In comparison with tissue culture plate (TCP), the cell viability remains above 95% with increasing the co-culture time (Figure 2g). The fluorescence images reveal that living cells (stained green) are evenly distributed in the hydrogel group (Figure 2h). The cell density increases significantly within 3 d. The direct attachment on the wrist skin for 3 d leads no signs of erythema, swelling, or allergic reactions (Figure 2i). These results suggest that the cellulose/MXene hydrogel is nontoxic and have good biocompatibility, which is mainly attributed to the low toxicity of cellulose and MXene.[20,21]

Strain Property of the cellulose/MXene Hydrogel Sensors

The strain sensing mechanism during the whole strain process is shown in Figure 3a. The geometric deformation under the tensile state leads to the increase of interval between MXene nanosheets due to their contact interfaces changing from surface-to-surface into surface-to-point or surface-to-edge. The reduced contact area in the hydrogel matrix extends the path of electronic conduction to increase the resistance.[35] Under the compression deformation, the resistance decreases as a result of the denser contact spacing between MXene nanosheets (Figure S9).[36] As an important parameter, sensitivity is assessed using gauge factor (GF). The relative resistance of C/M-0 hydrogel experiences a slow increase and the GF is 0.73 in the tensile strain range of 0–101% (Figure S10). Moreover, the GF of C/M-10 hydrogel increases to 1.52 in the tensile strain range of 0–140%. The cellulose/MXene hydrogel can not only serve as a reliable strain sensor under the tension state but also improve the tensile sensitivity. Then, the C/M-10 hydrogel exhibits more obviously sensitive electromechanical performance under the compression strain (Figure 3b). The relative resistance variation undergoes a sharp decrease as the compression deformation is less than 2%. The GF in the compression strain is -6.97 in the strain range of 0-2% and reduces to -1.32 between 2% and 19%, and reaches to −-0.35 when a higher strain is applied at 19-68%, which is significantly higher than the sensitivity of the C/M-0 hydrogel (Figure S11). The GF of -6.97 (0-2%) is higher than the strain sensor prepared by nano-carbon fiber/PVA hydrogel with the GF of 6.321 (0-10%).[37] The distance between adjacent MXene nanosheets rapidly decreases when the pressure is initially applied, which leads to the formation of direct contact between dispersed MXene nanosheets and a significant reduction in electrical resistance. With the further increase of deformation, most MXene nanosheets in direct contact are arranged in order, and the contact area and conductive paths are limited, resulting in a low sensitivity under a high compressive strain.[38] These results demonstrate that MXene uses as the nanofiller for cellulose hydrogel to promote the sensitivity of the cellulose/MXene hydrogel-based strain sensor. The relative resistance variation of the cellulose/MXene strain sensors under different strains (0–40%) is tested (Figure 3c). The strain sensor can distinguish different compression levels and maintain a stable sensing response. The response time of the device is up to 100 ms (Figure 3d), which ensures to detect the human motions in real-time. To test the minimum pressure detection limit, a series of round polyethylene gaskets with different pressures (i.e., 3, 6, 10, 15, 19, and 30 Pa) were placed on the piezoresistive sensors, respectively. The results show that the cellulose/MXene strain sensors could stably detect the pressure above 19 Pa in this detection device (Figure S12). After 1000 times of 40% compression strain, the signal output is stable and has no significant recession, showing a remarkable long-term durability and repeatability (Figure 3e).

Application of Strain Sensors

To achieve the real-time sensing monitor of the strain sensor, it is attached in different human body parts to detect the physiological signals and movement state of human motion (Video S2). During the movement of the fingers, elbows and wrists (Figure 4a-c), tensile deformation causes an increase in resistance and the change of relative resistance is proportional to the bending degree. In addition, the sensor can be attached to the corners of

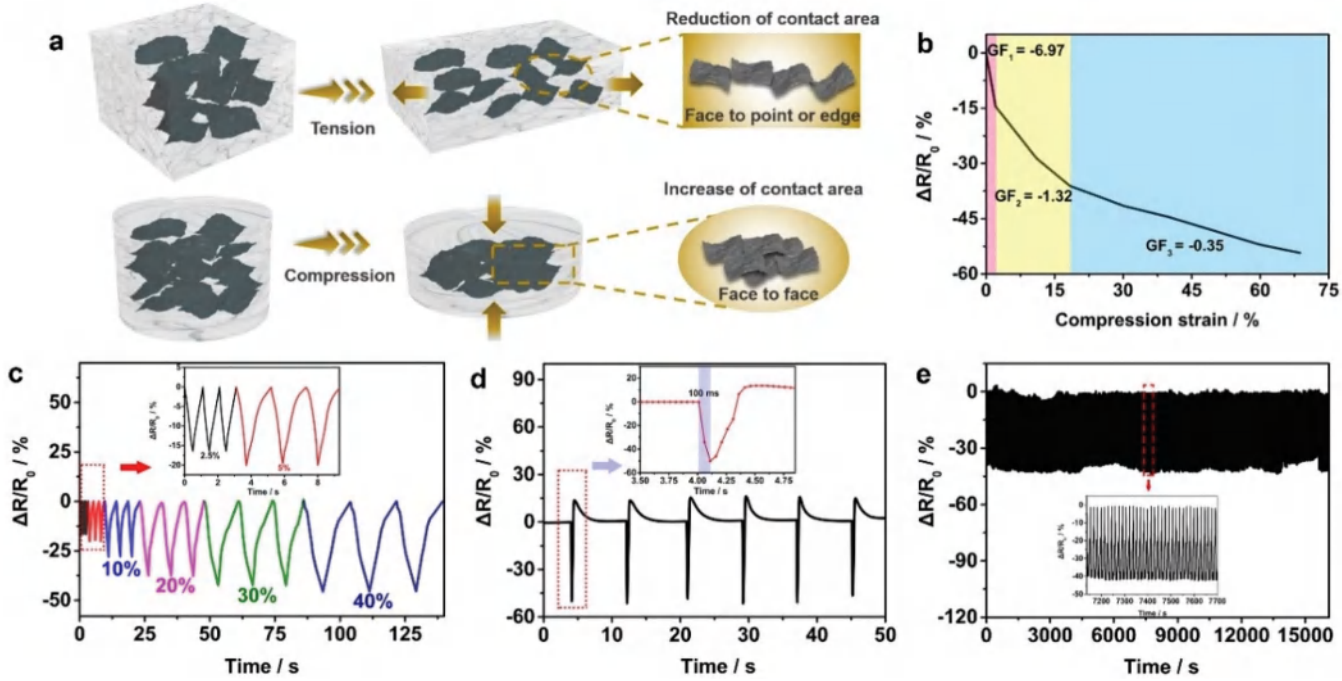

Figure 3. (a) Schematic diagram of electromechanical mechanism of hydrogel. (b) Relation between resistance variation and compression strain in strain sensor. (c) Relative resistance variation under different compression strains (2.5%, 5%, 10%, 20%, 30% and 40%). (d) Response time of the strain sensor under instantaneous compression. (e) Current stability of the strain sensor during 1000 cycles at 40% strain.

the mouth, throat, and wrist pulse to detect their subtle changes. The device detects the opening and closing movement of the mouth (Figure 4d). It can also accurately identify different monosyllabic and multi-syllable words (one, two, three and MXene) to use in speech recognition feedback system and deaf-mute auxiliary communication (Figure 4e). It can be used in speech recognition feedback system for human computer interaction and deaf-mute auxiliary communication. When the device is adhered to the arm pulse, regular and obvious pulse fluctuation signal is 78 times per minute, conforming the normal human heart rate (Figure 4f).[39] Apart from the large amplitude movement signals, it can also monitor the small deformation of physiological signals. A character recognition sensor can recognize single letters (i.e., g, e, and l) and the word (gel) (Figure 4g-j). The device has the real-time and accurate recognition for writing, which brings more possibilities for writing electronic products. A 4 × 4 sensor array platform based on cellulose/MXene hydrogel is fabricated for the human-computer interaction (Figure 4k). When the external pressure is exerted on the sensor surface, the contact points are precisely recognized through acquiring the sensing response of each pixel and drawing the sensing response 3D map with the pressure location and distribution (Figure 4l,m). It indicates that the cellulose/MXene hydrogel sensor arrays can be used as pressure sensing device and have potential application prospects in the field of human-computer interaction.

EMI Shielding Performance of Hydrogel

To shield the electromagnetic radiation, the EMI SE should be higher than 20 dB to shield the 90% of the electromagnetic waves.[40,41] The EMI SE of C/M-30 is 1.5 times higher than C/M-0 (15.4 dB) (Figure 5a). The EMI SE of hydrogel with thickness of 1, 2, 3, 4, and 5 mm is 13.8, 20.8, 24.3, 27.5, and 30 dB at 8.2 GHz, respectively (Figure 5c). They are higher than those in the previous works (Table S6). For C/M-30, SE_T, SE_A and SE_R are 22.8, 16.1, and 6.7 dB at 8.2 GHz, respectively (Figure 5b). The SE_T, SE_A and SE_R of C/M-10 with 5 mm-thick are 30, 21.8, and 8.2 dB at 8.2 GHz (Figure 5d), respectively. The EMI shielding mechanism of hydrogel is depicted in Figure 5e. When the electromagnetic wave touches the hydrogel, a small part of the electromagnetic wave is reflected, and the incident electromagnetic wave is dissipated by multiple reflections in the hydrogel, and some passes through the hydrogel.[24] From the SE ratio, the absorption-dominant electromagnetic shielding mechanism of hydrogel is speculated. Firstly, cellulose hydrogel matrix contributes to the uniform dispersion of MXene to build an efficient

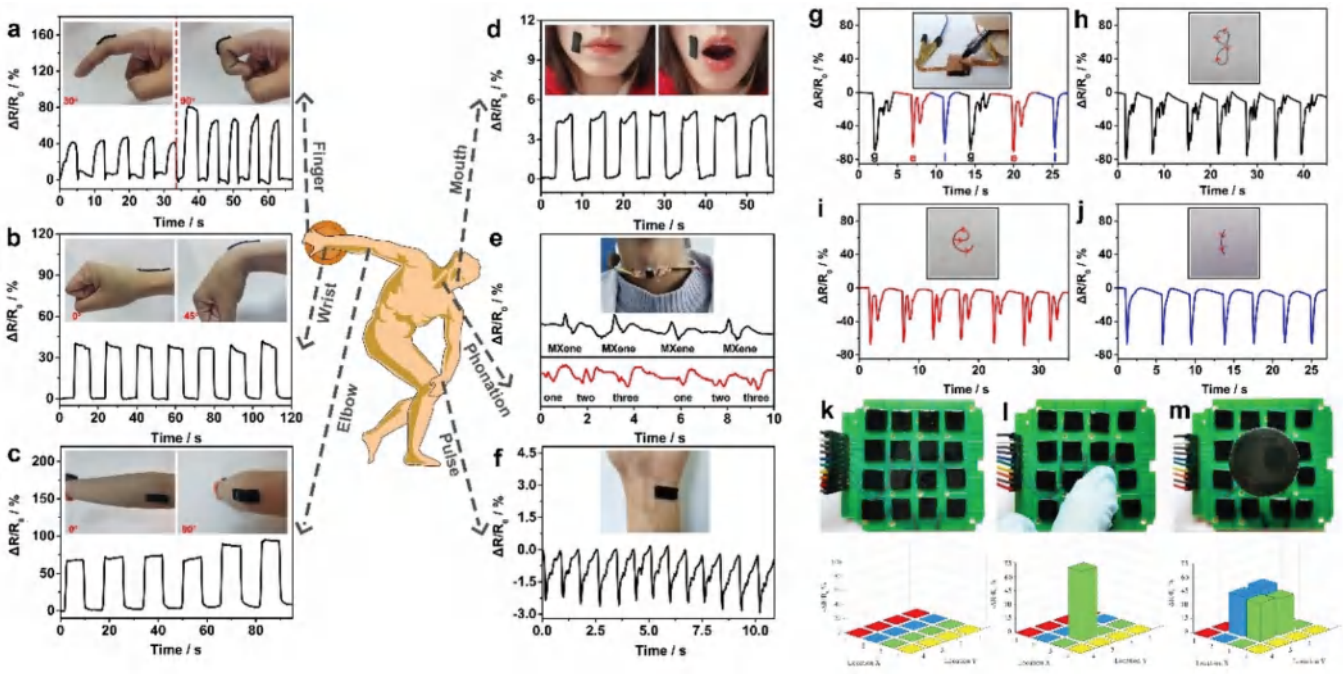

Figure 4. Applications of the cellulose/MXene hydrogel sensors for human motion detection. Real-time recording of the relative resistance changes generated by various human activities of finger (a), wrist (b), elbow (c), mouth (d), phonation (e) and pulse (f). Writing sensing applications of cellulose/MXene piezoresistive sensor. Resistance change caused by writing the phrase of gel (g), and a single word of g (h), e (i) and l (j). Photographs and 3D mapping of the pressure distribution of the 4 × 4 sensor array platform and assembled from C/M-10 hydrogel (k), a finger touching the hydrogel sensor (l) and a glass bottle placing in the sensor (m), respectively.

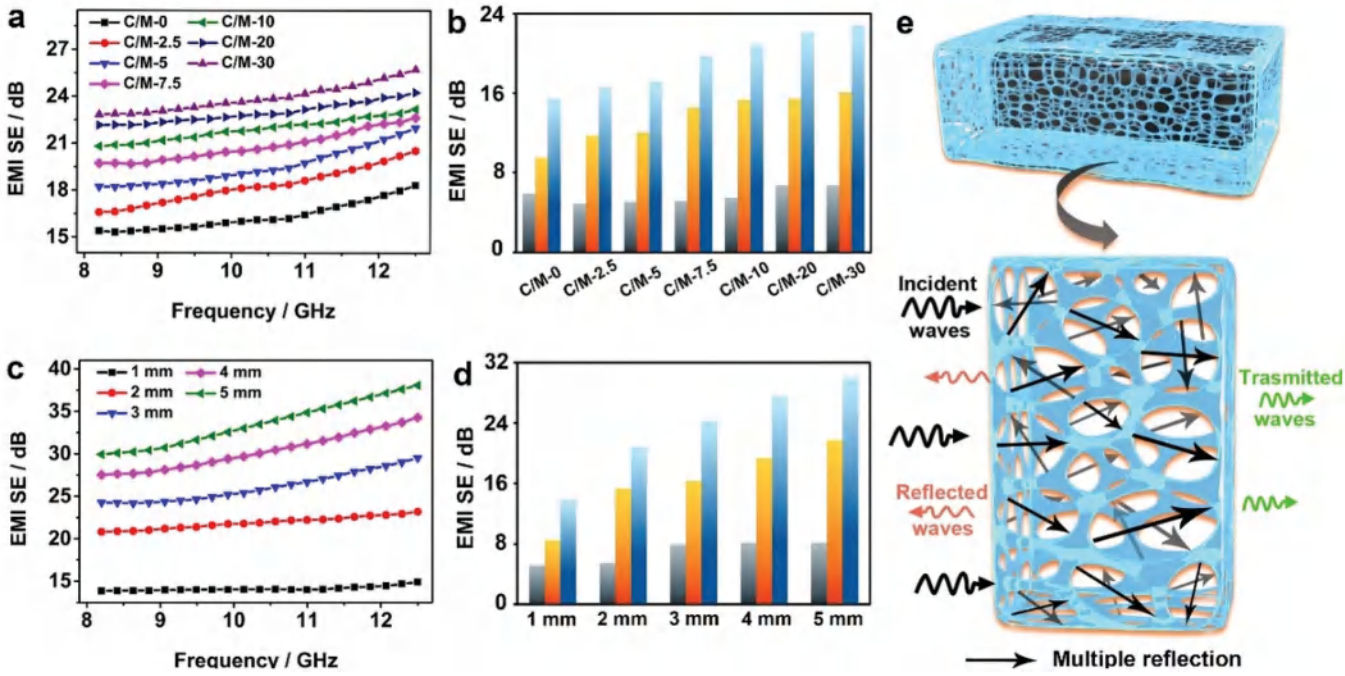

Figure 5. (a) EMI SE of hydrogel with different MXene loading in the frequency range of 8.2-12.4 GHz; (b) The SE_T, SE_A, and SE_R of hydrogel with different MXene loading at 8.2 GHz (c) EMI SE of hydrogel with different thickness. (d) The SE_T, SE_A, and SE_R of hydrogel with different thickness at 8.2 GHz (e) Schematic diagram of electromechanical mechanism of hydrogel.

conductive network. The SE_A boosts with the increase of MXene content due to the 2D sheet structure of MXene enhances the multiple reflection of electromagnetic wave inside and more conductive network acts as dissipative mobile charge carrier.[42] The surface functional groups of MXene nanosheets also effectively enhance the polarization losses to facilitate the attenuation of electromagnetic wave.[43] SE_R increases with the enhancement of conductivity and the movement of charge carrier. Then, the 3D porous structure of hydrogel provides a channel for incident wave and increases the internal multiple reflection attenuation.[44] Furthermore, the water in the hydrogel provides polarization loss and dielectric loss to further attenuate the electromagnetic wave.[45] At the same time, increasing the thickness of hydrogel can effectively enhance the EMI SE.

Conclusions

In summary, the biocompatible, stretchable, and compressible cellulose/MXene hydrogel has been fabricated for the dual functional applications of strain stress and EMI shielding. As a conductive filler, MXene is embedded into the 3D porous structure through hydrogen bond interaction with cellulose chain. Compared with cellulose hydrogel, the conductivity, and tensile properties of cellulose/MXene are increased by 1.6 times (14.9 mS m^{-1}) and 1.4 times (~144.4%). The strain sensor prepared by cellulose/MXene hydrogel with outstanding sensitivity compression response (GF = -6.97), fast response time (~100 ms), and good durability (~1000 cycles), which are better than that of nano-carbon fiber/PVA hydrogel etc. It realizes a real-time monitoring of the human activity, the character recognition and the pressure distribution of sensor array platform. In addition, due to the synergistic effect of appropriate conductivity, porous structure, and abundant water content, the hydrogel shows the EMI SE of 30 dB at 8.2 GHz, which is superior to that of most reported materials (Table S6). It paves an avenue to apply the cellulose/MXene hydrogel as the wearable electronics, intelligent robotics, human-computer interaction, and EMI shielding.

Acknowledgments

This work was supported by the National Funds for Distinguished Young Scientists (61825503), the National Natural Science Foundation of China (62174086), Postgraduate Research & Practice Innovation Program of Jiangsu Province (KYCX20_0755).

Disclosure statement

The authors declare that they have no known competing financial interests or personal relationships that could have appeared to influence the work reported in this paper.

Funding

This work was supported by the National Funds for Distinguished Young Scientists [61825503]; National Natural Science Foundation of China [62174086]; Postgraduate Research & Practice Innovation Program of Jiangsu Province [KYCX20_0755].

Author statement

The manuscript was written with contributions from all the authors. Yan Bai designed the project and performed the data, as well as wrote the manuscript. Shuaihang Bi, Weikang Wang, Ning Ding, Yuyuan Lu, Mengyue Jiang, and Chengbo Ding helped perform the analysis with constructive discussions. Weiwei Zhao conceived the idea and contributed to the conception of the study. Ning Liu designed the circuit and the software. Jing Bian and Shujuan Liu analyzed the data. Qiang Zhao provided comments and revised the manuscript. All authors contributed to the writing and revisions.

References

[1] Ates, H. C.; Yetisen, A. K.; Güder, F.; Dincer, C. Wearable Devices for the Detection of Covid-19. *Nat. Electron* 2021, 4(1), 13–14. DOI: 10.1038/s41928-020-00533-1.

[2] Gu, G.; Zhang, N.; Xu, H.; Lin, S.; Yu, Y.; Chai, G.; Ge, L.; Yang, H.; Shao, Q.; Sheng, X., et al. A Soft Neuroprosthetic Hand Providing Simultaneous Myoelectric Control and Tactile Feedback. *Nat. Biomed. Eng.* 2021. DOI: 10.1038/s41551-021-00767-0.

[3] Yeon, H.; Lee, H.; Kim, Y.; Lee, D.; Lee, Y.; Lee, J. S.; Shin, J.; Choi, C.; Kang, J. H.; Suh, J. M., et al. Long-Term Reliable Physical Health Monitoring by Sweat Pore-Inspired Perforated Electronic Skins. *Sci. Adv.* 2021, 7(27), 8459. DOI: 10.1126/sciadv.abg8459.

[4] Lee, S.; Franklin, S.; Hassani, F. A.; Yokota, T.; Nayeem, M. O. G.; Wang, Y.; Leib, R.; Cheng, G.; Franklin, D. W.; Someya, T. Nanomesh Pressure Sensor for Monitoring Finger Manipulation without Sensory Interference. *Science.* 2020, 370(6519), 966–970. DOI: 10.1126/science.abc9735.

[5] Shang, Y.; Wu, C.; Hang, C.; Lu, H.; Wang, Q. Hofmeister-Effect-Guided Ionohydrogel Design as Printable Bioelectronic Devices. *Adv. Mater.* 2020, 32(30), 2000189. DOI: 10.1002/adma.202000189.

[6] Li, M.; Chen, S.; Fan, B.; Wu, B.; Guo, X. Printed Flexible Strain Sensor Array for Bendable Interactive Surface. *Adv. Funct. Mater.* 2020, 30(34), 2003214. DOI: 10.1002/adfm.202003214.

[7] Liu, H.; Zhang, H.; Han, W.; Lin, H.; Li, R.; Zhu, J.; Huang, W. 3D Printed Flexible Strain Sensors: From Printing to Devices and Signals. *Adv. Mater.* 2021, 33 (8), 2004782. DOI: 10.1002/adma.202004782.

[8] Duan, Q.; Lu, Y. Silk Sericin as a Green Adhesive to Fabricate a Textile Strain Sensor with Excellent Electromagnetic Shielding Performance. *ACS Appl. Mater. Interfaces*. 2021, 13(24), 28832–28842. DOI: 10.1021/acsami.1c05671.

[9] Zhao, W.; Jin, B.; Wang, L.; Ding, C.; Jiang, M.; Chen, T.; Bi, S.; Liu, S.; Zhao, Q. Ultrathin Ti_3C_2 Nanowires Derived from Multi-Layered Bulks for High-Performance Hydrogen Evolution Reaction. *Chin. Chem. Lett.* 2021. DOI: 10.1016/j.cclet.2021.07.035.

[10] Naguib, M.; Kurtoglu, M.; Presser, V.; Lu, J.; Niu, J.; Heon, M.; Hultman, L.; Gogotsi, Y.; Barsoum, M. Two-Dimensional Nanocrystals: Two-Dimensional Nanocrystals Produced by Exfoliation of Ti_3AlC_2. *Adv. Mater.* 2011, 23, 4207-4207. DOI: 10.1002/adma.201190147.

[11] Gao, L.; Bao, W.; Kuklin, A. V.; Mei, S.; Zhang, H.; Ågren, H. Hetero-MXenes: Theory, Synthesis, and Emerging Applications. *Adv. Mater.* 2021, 33(10), 2004129. DOI: 10.1002/adma.202004129.

[12] Zhang, Y.; Jiang, X.; Zhang, J.; Zhang, H.; Li, Y. Simultaneous Voltammetric Determination of Acetaminophen and Isoniazid Using MXene Modified Screen-Printed Electrode. *Biosens. Bioelectron.* 2019, 130, 315–321. DOI: 10.1016/j.bios.2019.01.043.

[13] Jiang, X.; Li, W.; Hai, T.; Yue, R.; Chen, Z.; Lao, C.; Ge, Y.; Xie, G.; Wen, Q.; Zhang, H. Inkjet-Printed MXene Micro-Scale Devices for Integrated Broadband Ultrafast Photonics. *NPJ 2D Mater. Appl.* 2019, 3(1), 34. DOI: 10.1038/s41699-019-0117-3.

[14] Huang, W.; Hu, L.; Tang, Y.; Xie, Z.; Zhang, H. Recent Advances in Functional 2D MXene-Based Nanostructures for Next-Generation Devices. *Adv. Funct. Mater.* 2020, 30(49), 2005223. DOI: 10.1002/adfm.202005223.

[15] Luo, X.; Zhu, L.; Wang, Y. C.; Li, J.; Nie, J.; Wang, Z. L. A Flexible Multifunctional Triboelectric Nanogenerator Based on MXene/PVA Hydrogel. *Adv. Funct. Mater.* 2021, 31(38), 2104928. DOI: 10.1002/adfm.202104928.

[16] Cheng, Y.; Ma, Y.; Li, L.; Zhu, M.; Yue, Y.; Liu, W.; Wang, L.; Jia, S.; Li, C.; Qi, T., et al. Bioinspired Microspines for a High-Performance Spray $Ti_3C_2T_x$ MXene-Based Piezoresistive Sensor. *ACS Nano*. 2020, 14(2), 2145–2155. DOI: 10.1021/acsnano.9b08952.

[17] Guo, J.; Yu, Y.; Zhang, H.; Sun, L.; Zhao, Y. Elastic MXene Hydrogel Microfiber-Derived Electronic Skin for Joint Monitoring. *ACS Appl. Mater. Interfaces*. 2021, 13(40), 47800–47806. DOI: 10.1021/acsami.1c10311.

[18] Zolfaghari, N.; Moghimi Zand, M.; Mofrad, M. R. K. Strain-Stiffening and Strain-Softening Responses in Random Viscoelastic Fibrous Networks: Interplay between Fiber Orientation and Viscoelastic Softening. *Soft Mater.* 2020, 18(4), 373–385. DOI: 10.1080/1539445X.2019.1697705.

[19] Stancu, I. C.; Lungu, A.; Dragusin, D. M.; Vasile, E.; Damian, C.; Iovu, H. Porous Gelatin-Alginate-Polyacrylamide Scaffolds with Interpenetrating Network Structure: Synthesis and Characterization. *Soft Mater.* 2013, 11(4), 384–393. DOI: 10.1080/1539445X.2011.642091.

[20] Mao, L.; Hu, S.; Gao, Y.; Wang, L.; Zhao, W.; Fu, L.; Cheng, H.; Xia, L.; Xie, S.; Ye, W., et al. Biodegradable and Electroactive Regenerated Bacterial Cellulose/MXene ($Ti_3C_2T_x$) Composite Hydrogel as Wound Dressing for Accelerating Skin Wound Healing under Electrical Stimulation. *Adv. Healthc. Mater* 2020, 9(19), 2000872. DOI: 10.1002/adhm.202000872.

[21] Xing, C.; Chen, S.; Liang, X.; Liu, Q.; Qu, M.; Zou, Q.; Li, J.; Tan, H.; Liu, L.; Fan, D., et al. Two-Dimensional MXene (Ti_3C_2)-Integrated Cellulose Hydrogels: Toward Smart Three-Dimensional Network Nanoplatforms Exhibiting Light-Induced Swelling and Bimodal Photothermal/Chemotherapy Anticancer Activity. *ACS Appl. Mater. Interfaces*. 2018, 10(33), 27631–27643. DOI: 10.1021/acsami.8b08314.

[22] Chen, K.; Zong, T.; Chen, Q.; Liu, S.; Xu, L.; Zhang, D. Preparation and Characterization of Polyvinyl Alcohol/Sodium Alginate/Carboxymethyl Cellulose Composite Hydrogels with Oriented Structure. *Soft Mater.* 2022, 20(1), 99–108. DOI: 10.1080/1539445X.2021.1926281.

[23] Zhu, Y.; Liu, J.; Guo, T.; Wang, J. J.; Tang, X.; Nicolosi, V. Multifunctional $Ti_3C_2T_x$ MXene Composite Hydrogels with Strain Sensitivity toward Absorption-Dominated Electromagnetic-Interference Shielding. *ACS Nano*. 2021, 15(1), 1465–1474. DOI: 10.1021/acsnano.0c08830.

[24] Yang, W.; Shao, B.; Liu, T.; Zhang, Y.; Huang, R.; Chen, F.; Fu, Q. Robust and Mechanically and Electrically Self-Healing Hydrogel for Efficient Electromagnetic Interference Shielding. *ACS Appl. Mater. Interfaces*. 2018, 10(9), 8245–8257. DOI: 10.1021/acsami.7b18700.

[25] Ruiz Perez, F.; López Estrada, S. M.; Tolentino Hernández, R. V.; Caballero Briones, F. Carbon-Based, Radar Absorbing Materials: A Critical Review. *J. Sci. Adv. Mater. Dev*. 2022, 100454. DOI: 10.1016/j.jsamd.2022.100454.

[26] Shahzad, F.; Alhabeb, M.; Hatter, C. B.; Anasori, B.; Hong, S. M.; Koo, C. M.; Gogotsi, Y. Electromagnetic Interference Shielding with 2D Transition Metal Carbides (Mxenes). *Science*. 2016, 353(6304), 1137–1140. DOI: 10.1126/science.aag2421.

[27] Yue, Y.; Liu, N.; Ma, Y.; Wang, S.; Liu, W.; Luo, C.; Zhang, H.; Cheng, F.; Rao, J.; Hu, X., et al. Highly Self-Healable 3D Microsupercapacitor with MXene-Graphene Composite Aerogel. *ACS Nano*. 2018, 12(5), 4224–4232. DOI: 10.1021/acsnano.7b07528.

[28] Ye, D.; Yang, P.; Lei, X.; Zhang, D.; Li, L.; Chang, C.; Sun, P.; Zhang, L. Robust Anisotropic Cellulose Hydrogels Fabricated via Strong Self-Aggregation Forces for Cardiomyocytes Unidirectional Growth. *Chem. Mater.* 2018, 30(15), 5175–5183. DOI: 10.1021/acs.chemmater.8b01799.

[29] Zhang, P.; Yang, X.; Li, P.; Zhao, Y.; Niu, Q. J. Fabrication of Novel MXene (Ti_3C_2)/Polyacrylamide Nanocomposite Hydrogels with Enhanced Mechanical and Drug Release Properties. *Soft Matter*. 2020, 16(1), 162–169. DOI: 10.1039/C9SM01985E.

[30] Tong, R.; Chen, G.; Pan, D.; Qi, H.; Li, R. A.; Tian, J.; Lu, F.; He, M. Highly Stretchable and Compressible Cellulose Ionic Hydrogels for Flexible Strain Sensors. *Biomacromolecules*. 2019, 20(5), 2096–2104. DOI: 10.1021/acs.biomac.9b00322.

[31] Chen, C.; Duan, N.; Chen, S.; Guo, Z.; Hu, J.; Guo, J.; Chen, Z.; Yang, L. Synthesis Mechanical Properties and Self-Healing Behavior of Aliphatic Polycarbonate Hydrogels Based on Cooperation Hydrogen Bonds. *J. Mol. Liq.* 2020, 319, 114134. DOI: 10.1016/j.molliq.2020.114134.

[32] Liao, H.; Guo, X.; Wan, P.; Yu, G. Conductive MXene Nanocomposite Organohydrogel for Flexible, Healable, Low-Temperature Tolerant Strain Sensors. *Adv. Funct. Mater.* 2019, 29(39), 1904507. DOI: 10.1002/adfm.201904507.

[33] Wang, Q.; Pan, X.; Wang, X.; Gao, H.; Chen, Y.; Chen, L.; Ni, Y.; Cao, S., and Ma, X. Spider Web-Inspired Ultra-Stable 3D $Ti_3C_2T_x$ (MXene) Hydrogels Constructed by Temporary Ultrasonic Alignment and Permanent in-Situ Self-Assembly Fixation. *Compos. Part B: Eng.* 2020, 197, 108187. DOI: 10.1016/j.compositesb.2020.108187.

[34] Jiao, Y.; Lu, K.; Lu, Y.; Yue, Y.; Xu, X.; Xiao, H.; Li, J.; Han, J. Highly Viscoelastic,Stretchable, Conductive, and Self-Healing Strain Sensors Based on Cellulose Nanofiber-Reinforced Polyacrylic Acid Hydrogel. *Cellulose*. 2021, 28, 4295–4311. DOI: 10.1007/s10570-021-03782-1.

[35] Yuan, W.; Qu, X.; Lu, Y.; Zhao, W.; Ren, Y.; Wang, Q.; Wang, W.; Dong, X. MXene-Composited Highly Stretchable, Sensitive and Durable Hydrogel for Flexible Strain Sensors. *Chin. Chem. Lett.* 2020, 32(6), 2021–2026. DOI: 10.1016/j.cclet.2020.12.003.

[36] Gao, Y.; Yan, C.; Huang, H.; Yang, T.; Tian, G.; Xiong, D.; Chen, N.; Chu, X.; Zhong, S.; Deng, W., et al. Microchannel-Confined MXene Based Flexible Piezoresistive Multifunctional Micro-Force Sensor. *Adv. Funct. Mater.* 2020, 30(11), 1909603. DOI: 10.1002/adfm.201909603.

[37] Cheng, B.; Chang, S.; Li, H.; Li, Y.; Shen, W.; Shang, Y.; Cao, A. Highly Stretchable and Compressible Carbon Nanofiber-Polymer Hydrogel Strain Sensor for Human Motion Detection. *Macromol. Mater. Eng.* 2020, 305(3), 1900813. DOI: 10.1002/mame.201900813.

[38] Wang, Z.; Chen, J.; Wang, L.; Gao, G.; Zhou, Y.; Wang, R.; Xu, T.; Yin, J.; Fu, J. Flexible and Wearable Strain Sensors Based on Tough and Self-Adhesive Ion Conducting Hydrogels. *J. Mater. Chem. B*. 2019, 7(1), 24–29. DOI: 10.1039/C8TB02629G.

[39] Jiang, D.; Zhang, J.; Qin, S.; Wang, Z.; Usman, K. A. S.; Hegh, D.; Liu, J.; Lei, W.; Razal, J. M. Superelastic $Ti_3C_2T_x$ MXene-Based Hybrid Aerogels for Compression-Resilient Devices. *ACS Nano*. 2021, 15(3), 5000–5010. DOI: 10.1021/acsnano.0c09959.

[40] Liu, J.; Zhang, H. B.; Sun, R.; Liu, Y.; Liu, Z.; Zhou, A.; Yu, Z. Z. Hydrophobic, Flexible, and Lightweight MXene Foams for High-Performance Electromagnetic-Interference Shielding. *Adv. Mater.* 2017, 29(38), 1702367. DOI: 10.1002/adma.201702367.

[41] Cao, M. S.; Wang, X. X.; Cao, W. Q.; Yuan, J. Ultrathin Graphene: Electrical Properties and Highly Efficient Electromagnetic Interference Shielding. *J. Mater. Chem. C*. 2015, 3(26), 6589–6599. DOI: 10.1039/C5TC01354B.

[42] Zeng, Z.; Chen, M.; Jin, H.; Li, W.; Xue, X.; Zhou, L.; Pei, Y.; Zhang, H.; Zhang, Z. Thin and Flexible Multi-Walled Carbon Nanotube/Waterborne Polyurethane Composites with High-Performance Electromagnetic Interference Shielding. *Carbon*. 2016, 96, 768–777. DOI: 10.1016/j.carbon.2015.10.004.

[43] Iqbal, A.; Shahzad, F.; Hantanasirisakul, K.; Kim, M. K.; Kwon, J.; Hong, J.; Kim, H.; Kim, D.; Gogotsi, Y.; Koo, C. M. Anomalous Absorption of Electromagnetic Waves by 2D Transition Metal Carbonitride (Mxene). *Science*. 2020, 369(6502), 446–450. DOI: 10.1126/science.aba7977.

[44] Liu, X.; Jin, X.; Li, L.; Wang, J.; Yang, Y.; Cao, Y.; Wang, W. Air-Permeable, Multifunctional, Dual-Energy-Driven MXene-Decorated Polymeric Textile-Based Wearable Heaters with Exceptional Electrothermal and Photothermal Conversion Performance. *J. Mater. Chem. A*. 2020, 8(25), 12526–12537. DOI: 10.1039/D0TA03048A.

[45] Song, W. L.; Zhang, Y. J.; Zhang, K. L.; Wang, K.; Zhang, L.; Chen, L. L.; Huang, Y.; Chen, M.; Lei, H.; Chen, H., et al. Ionic Conductive Gels for Optically Manipulatable Microwave Stealth Structures. *Adv. Sci*. 2020, 7(2), 1902162. DOI: 10.1002/advs.201902162.